Open Journal of Geology, 2022, 12, 333-357
https://www.scirp.org/journal/ojg
ISSN Online: 2161-7589
ISSN Print: 2161-7570

Lineaments Extraction and Analysis Using Landsat 8 (OLI/TIRS) in the Northeast of Morocco

Meryem Redouane[1], Hicham Si Mhamdi[2], Faouziya Haissen[1], Mohammed Raji[1], Othman Sadki[3]

[1]LGAGE, Faculty of Sciences Ben M'sik, Hassan II University of Casablanca, Casablanca, Morocco
[2]LAG, Faculty of Sciences and Techniques, Moulay Ismaïl University, Errachidia, Morocco
[3]National Office of Hydrocarbons and Mines, Rabat, Morocco
Email: meryem.redouane.2015@gmail.com

How to cite this paper: Redouane, M., Mhamdi, H.S., Haissen, F., Raji, M. and Sadki, O. (2022) Lineaments Extraction and Analysis Using Landsat 8 (OLI/TIRS) in the Northeast of Morocco. *Open Journal of Geology*, **12**, 333-357.
https://doi.org/10.4236/ojg.2022.125018

Received: April 11, 2022
Accepted: May 24, 2022
Published: May 27, 2022

Abstract

Northeastern Morocco is made up of several units belonging to the Alpine belt and its foreland. Miocene to plio-quaternary volcanic rocks with variable mineralogy and geochemistry dominate the geology of this region. The presence of active faults in different directions explains the high tectonic instability and the high frequency of earthquakes. This study contributes to the effort of understanding the geothermal potential of the Northeast of Morocco. Heat source and permeability are both key factors in the geothermal process. Indeed, lineaments analysis constrains the structures and their directions and indicates severely faulted zones, which are the most promising areas for geothermal exploration. For this purpose, we used Landsat data combined with geological and structural maps available in this region. Different image processing techniques were applied including band ratio (6/2) and directional filters. To validate the results, we conducted a comparative study between linear structures, available geological data, and previous studies. Results of the automatic extraction method of lineaments from Landsat 8 OLI/TIRS indicate three main lineament systems: 1) a NE-SW system ranging from N40 to N70; 2) an N-S system ranging from N10 to N45; 3) an EW to WNW-ESE systems ranging from N80 to N120. Most of lineaments extracted are localized in Kebdana, Amejjaou, Nador and Melilla regions. Compared to previous studies, the NE-SW system is consistent with an extensive period (Tortonian to Pliocene); the NW-SE system is consistent with the last compressive episode (Pliocene); the N-S system is consistent with the first compressive period (Late/End Tortonian).

Keywords

Northeastern Morocco, Rif Belt, Faults, Miocene-Plio Quaternary Volcanism, Permeability, Lineaments, Landsat 8 (OLI/TIRS)

1. Introduction

In the last few years, remote sensing has been a very promising tool for researchers in different disciplines, including mining exploration [1] [2] [3] [4] and geological mapping ([5] [6] [7] and references therein). Many approaches were developed with the aim of identifying morphological and structural lineaments [8]-[28]. Such methods use geomorphologic signatures deduced from high spatial resolution images, such as Landsat ETM+, OLI/TIRS, and Sentinel. Three main lineament interpretation methods are usually adopted as follows: manual lineament interpretation, automatic lineament extraction and semi-automatic extraction. The visual interpretation consists of textural patterns related to geomorphological features and tonal contrast [29] [30] while the automatic extraction uses computer algorithms. Image enhancement and filtering options are applied to processed images with different image processing techniques, for instance, Principal Component Analysis (PCA) and band ratio (e.g. [31] [32] [33] [34]). The processing for lineament extraction purposes is usually performed on grey-colour spanning images instead of colored images because it gives better results as the contrast is better exposed in black and white versions [35]. The filters are chosen afterward and applied using software (e.g. Geomatica), which can be either directional [31] [32] non-directional [30] [36] or both [37] [38]. A recent study [39] has questioned both filtering techniques while extracting lineaments and got better results with directional filtering compared to non-directional filtering. However, the application of direction filters may produce some artefacts [40], which can be confusing, and should be corrected and revised. To minimize the errors resulting from visual interpretation, several authors [41] [42] suggest doing the same process several times with a week break at least and then comparing it with interpretations of the same operation of another observer.

The northeast of Morocco consists of two orogenic belts, the Rif chain in the north and an intracontinental belt called the Atlas, developed within the alpine tectonic foreland [43], to the south. The study area borders the junction between these domains, where three structural units directed ENE-WSW were previously identified [44]: 1) the eastern-rifian foreland; 2) Guercif and Taourirt-Oujda basins; 3) Taourirt-Oujda mounts. They exhibit complicated tectonic features showing both compressive and extensional structures, dated from Miocene to Plio-quaternary. The hercynian basement outcrops near the Taourirt-Oujda area and the deformation is concentrated in the shear zones, striking ENE-WSW to E-W [45] [46]. The faults used the pre-existent structures and reactivated them during the Late Triassic period, which mainly consisted of red mudstones, carbonates and tholeiitic basalts [47]. A carbonate platform was developed in the Early Liassic, and was cut later by a series of extensional faults forming a pattern of grabens and horsts oriented ENE-WSW and E-W. Then, a major NNW-SSE extension occurred between the Jurassic and the Early Cretaceous [48]. This extension was followed by a long compressive event, which started in the Eocene and created the NW-SE and NNE-SSW strike-slip faults and the E-W folds, and persisted to the Miocene [48] when volcanism took place.

The study area is known for a Plio-quaternary volcanic activity and a large number of geothermal manifestations (**Figure 1**). The lack of subsurface imaging data in geothermal areas encourages geologists to acquire more surface information and infer the subsurface geologic conditions (e.g. mineral alteration, permeability…). Lineaments, as extractable geological features, refer to rock fractures, joints and faults. The latter plays a key role in creating the porosity and permeability, which allows the capture and storage of thermal fluids in a geothermal system. Thus, characterizing these features shall contribute significantly to the understanding of the fluids' behaviour in a geothermal reservoir. In this paper, we applied the automatic extraction method using a Landsat8 (OLI/TIRS) image, covering northeastern Morocco, then, we applied the visual inspection to add and remove lineaments in order to construct a map of tectonic lineaments. The results are remarkably important as they demonstrate that the automatic extraction method can indicate the presence of small fractures, hardly detected in the field, their global directions and density and hence can be a good prospect for permeability.

2. Geological Settings

Rif-Tell belt is an Alpine system, resulting from the progressive closure of the Maghrebian Tethys and slab rollback of its lithosphere since the late Eocene [49]. The Rif belt (**Figure 1(b)**) forms the westernmost part of the alpine belt, which extends along the north of Africa (with Tell and Kabylia) and continues eastward to Sicily and Calabria in southern Italy. The Rif belt consists of three structural and paleogeographic domains: Internal Zones, Flysch Zones and External Zones. Morocco is located in the northwesternmost part of Africa overlooking the Mediterranean Sea to the north and the Atlantic Ocean to the west (**Figure 1(a)**).

The studied region corresponds to northeastern Morocco, made up of several units from the Rif belt and its foreland. The geological setting is marked by the presence of four main volcanic areas, displaying different mineralogy, geochemistry and age: A calc alkaline/shoshonitic volcanism dated at 13.1 - 4.8 Ma; alkaline volcanism dated at 6.3 Ma - 0.88 Ma with transitional terms occurring between 6.3 Ma and 4.8 Ma (first alkali basalt to latest Shoshonite, respectively) [50]. The high tectonic instability within the region is due to the presence of many faults in different directions. Recent geophysical explorations demonstrate that the lithosphere

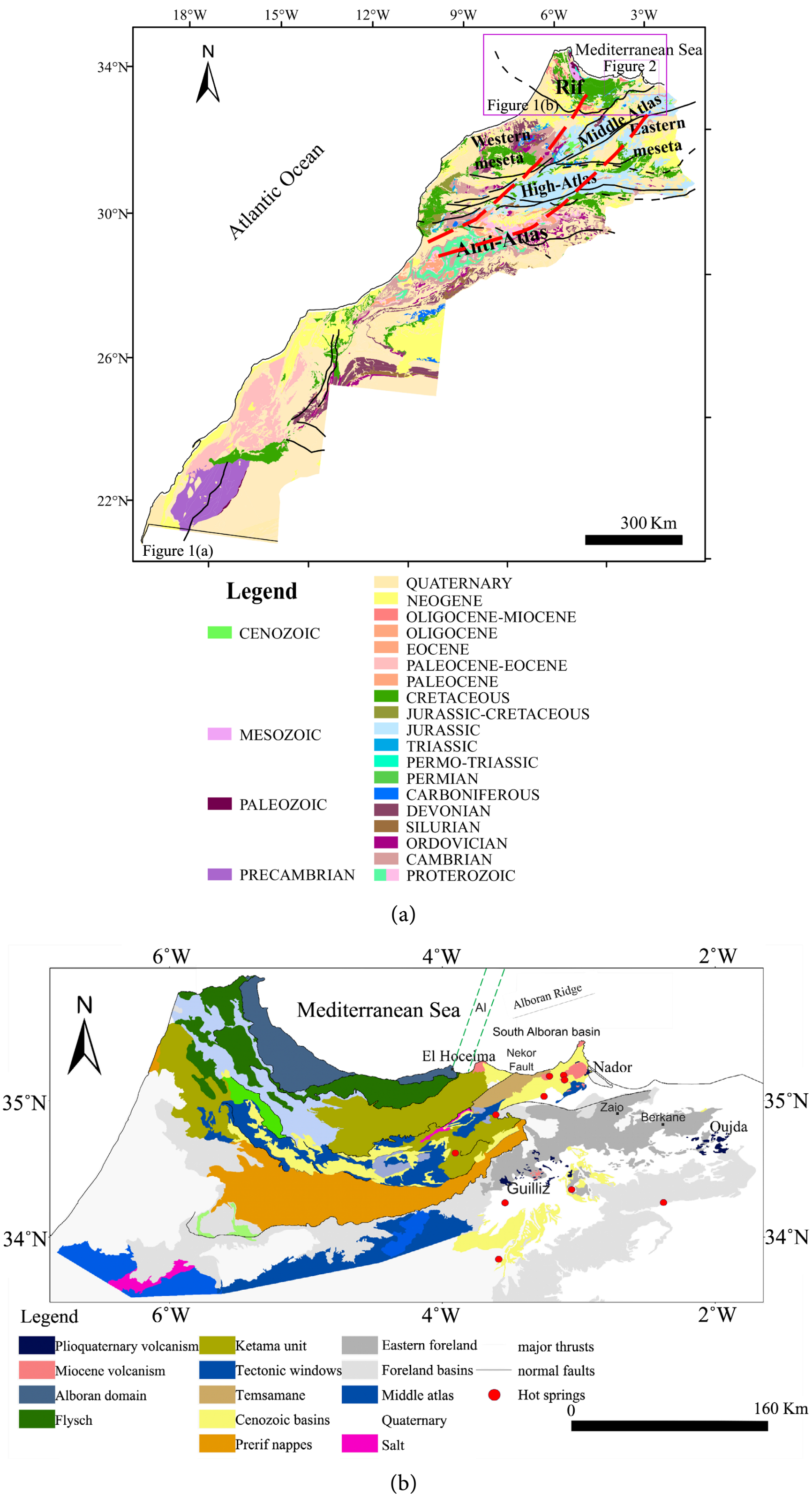

(a)

(b)

Figure 1. Regional geological settings ((a) geological map of Morocco, red dotted lines represent the Moroccan Hot Line; (b) the main structural domains of the Rif belt [57], green dotted lines corresponds to the Al-idrissi Fault zone (AI) [58] and red circles refer to the distribution of hot springs within the NE area).

beneath NE Morocco is anomalously thinned extending far to the South (Agadir) [51], delineating what is called "The Moroccan hot line" defined by [52] (**Figure 1(a)**). The Tertiary alkaline volcanism observed within the area in Gourougou (Nador), Guilliz (Guercif) and Oujda volcanic provinces is related to this hot line. This volcanism is also reported in the Middle Atlas (the most important province) and in the Anti-Atlas (Siroua and Saghro) [53] [54], where high magnetic anomalies were found [55]. Many tectonic models were proposed to discuss their origin (e.g. [50] [52] [53] [54] [56]), however, the relationship between different volcanic episodes is still a matter of debate.

On one hand, the presence of NE-SW major strike-slip faults and structures crossing from Agadir to the High and Middle Atlas, associated with faults in the eastern Rif (Nekor) led many authors [53] [59] [60] to suggest a fault system referred as "en echelon". Most of those faults cross the Alboran Sea and link up with the easternmost part of the Betics [61].

On the other hand, the Eastern Morocco volcanism is settled on Upper Miocene sedimentary basins [53]. Many authors [62] suggested subduction as the main cause of this magmatic activity; however, this hypothesis could not be corroborated because of the lack of any chronological or geochemical polarity. Thus, the model of a transverse strike-slip system, occurring between Iberia and Africa, linking both crusts and affecting the entire lithosphere, was highly recommended by [63] and supported by geochemical data (e.g. [50] [54] [64]). Results showed that Neogene magmatic activity is predominantly related to an extensional regime created by the upwelling of a mantle source, enriched during the previous subduction, while the Plio-quaternary volcanism is related to a compressional system, with an enriched lithospheric mantle source and a possible asthenospheric depleted mantle.

The compressional stress regime in Northeast of Morocco displayed since Tortonian volcanic activity three sedimentary and eruptive bodies (**Figure 1**), these elements recorded the chronology of tectonic events [65] [66]:

- The first is a N40 compressive stress trend is responsible for the development of Tortonian basins. Kebdana and Temsamane basins are developed along strike-slip faults oriented N70 - N90, while N-S and N40 - 50 trends are responsible for forming Boudinar and Nekor basins, respectively. Calc-alkaline volcanism of Ras Tarf and Trois Fourches is associated with the basins of Boudinar and Nekor [67].
- The second is a compressive stress-oriented N-S and occurs in late Tortonian and during the Messinian. A reverse movement is registered along N90 faults in addition to strike-slip movement on faults striking N70, N40 - 50 and N-S. Those movements were the expression of a variation in paleostress direction and led to the development of Guercif, Boudinar and Kert basins [61] [67]. The E-W extension in the Northeast of Morocco is responsible for normal faults, oriented N-S, frequently exposed all over the post-nappes basins. This event was synchronous with shoshonitic volcanic eruptions in Nador and Guercif regions (Gourougou and Guilliz) [53].

- The third consists of a counterclockwise rotation of the stress field with a max. Compressive stress-oriented N140 - 160 [66], N90 and N120 - 140 structures are mainly dextral strike-slip faults while the N-S structures are sinistral. Faults oriented N40 - 70 are reactivated with a sinistral behaviour [67]. Previous studies (e.g. [61] [65] [66] [68]-[73]) recorded that this compressive stress (N140 - 160) has been well identified all over the Northeast of Morocco (from Rif basins to middle and high Atlas). The alkaline activity took place during the same period in the eastern Rif and its foreland [53] [74].

The split of several blocks showing an alternation of horst and troughs has characterized the Neotectonic evolution of Northeast of Morocco. Compressive and extensive stress regimes at this time were associated simultaneously [67]. Different structures presented in Northeast of Morocco (**Figure 2**), including the numerous volcanic intrusions (veins, eruptive centres, etc.) feeding the lava flows, are formed following three major directions: NE-SW, NW-SE and N-S. Consequently, volcanic emissions seem to be parallel to faults trending N70 - 90, N40 - 50 and N-S, dominating the area's structure; N120 - 140 faults are locally associated [67].

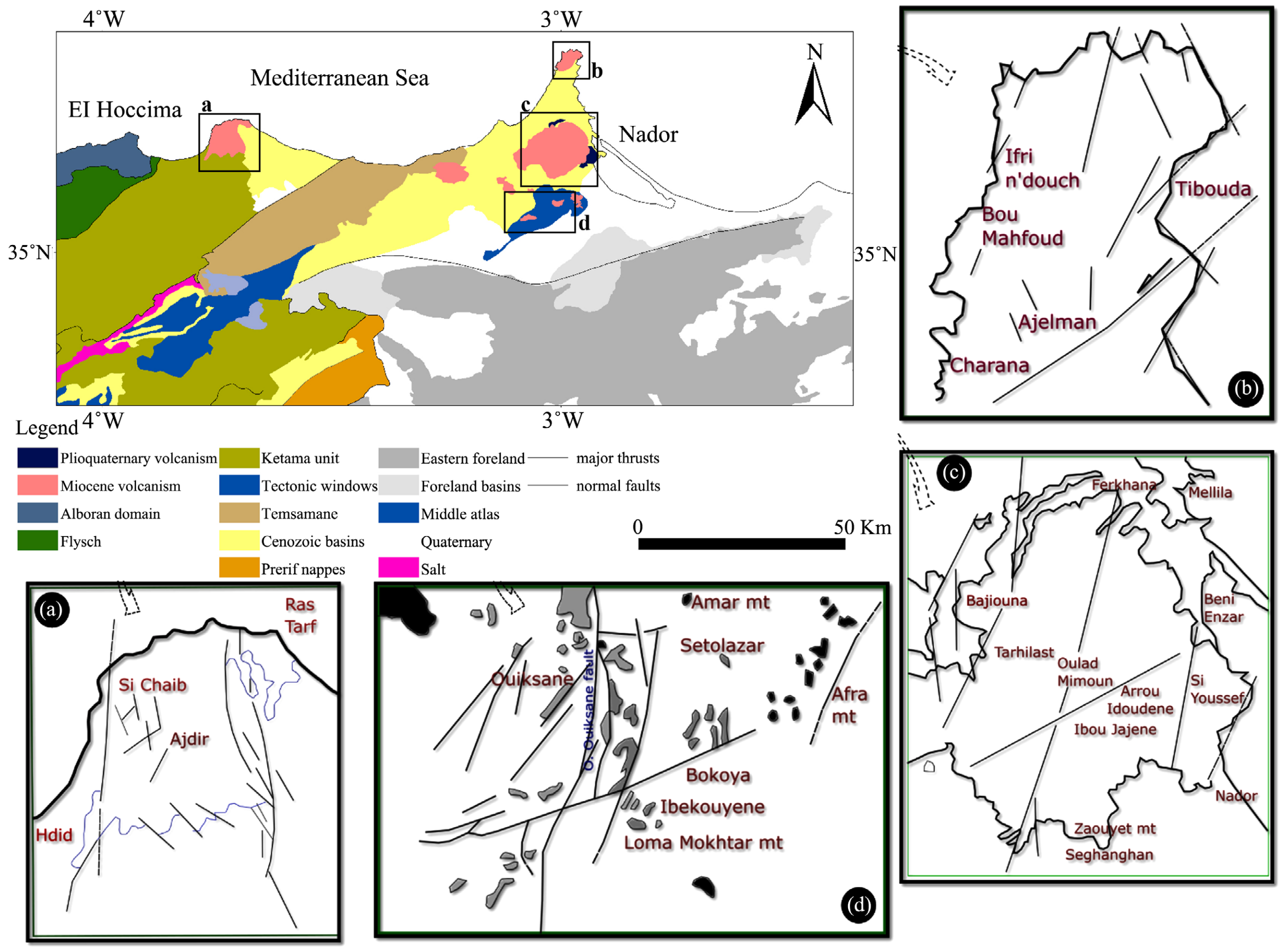

Figure 2. Geological map of Eastern Rif (Morocco) with the distribution of volcanism in the Neogene basin, after [75]. (a) Ras Tarf, (b) Trois fourches, (c) Gourougou, (d) Beni Bou Ifrour [67].

3. Materials and Methods

3.1. Data

In this paper, we work on Northeast of Morocco. The image used is landsat8 OLI/TIRS (Path 201 and Row 36, taken on 9th January 2019) and the data is available free at the United States Geological Survey website (https://earthexplorer.usgs.gov). It is provided with the Universal Transverse Mercator (UTM) projection and a WGS 84 World Geodetic System. This image contains eleven bands with different wavelengths and resolutions (**Table 1**) from Landsat 8 image. The most used band in geology are the optical bands (OLI) from the Coastal aerosol to the panchromatic band. In order to validate the results, we used as references the maps covering the study area at different scales (The Neotectonic map 1/1,000,000 (1994); The geological map of Kebdani: 1/50,000 (1984) The geological map of Berkane 1/50,000 (2001); The geological map of Zaio 1/50,000 (authors, 2001); The geological map of Seghanghan 1/50,000) (1996).

3.2. Methods

The main step of lineament extraction is described in the following chart (**Figure 3**). It starts with pre-processing, consisting of radiometric and atmospheric corrections, then the processing, to enhance the visibility of lineaments in the images. The main purpose is to identify lineaments with possible structural origins. After several attempts using different image processing techniques, classifications and colour composite images, we concluded that linear structures are more visible in the 6/2 band ratio images, the choice is also supported by other studies (e.g. [78]). Hence, the ratio of 6/2 image was sharpened and directional filters were applied (**Figure 3**).

Table 1. Spectral bands of the Landsat 8 satellite [76] [77].

Bands		Wavelengths (μm)	Spatial resolution (m)
Band 1	Coastal aerosol	0.43 to 0.45	30
Band 2	Blue	0.45 to 0.51	30
Band 3	Green	0.53 to 0.59	30
Band 4	Red	0.64 to 0.67	30
Band 5	NIR	0.85 to 0.88	30
Band 6	SWIR1	1.57 to 1.65	30
Band 7	SWIR2	2.11 to 2.29	30
Band 8	Panchromatic	0.50 to 0.68	15
Band 9	Cirrus	1.36 to 1.38	30
Band 10	TIRS1	10.60 to 11.19	100
Band 11	TIRS2	11.50 to 12.51	100

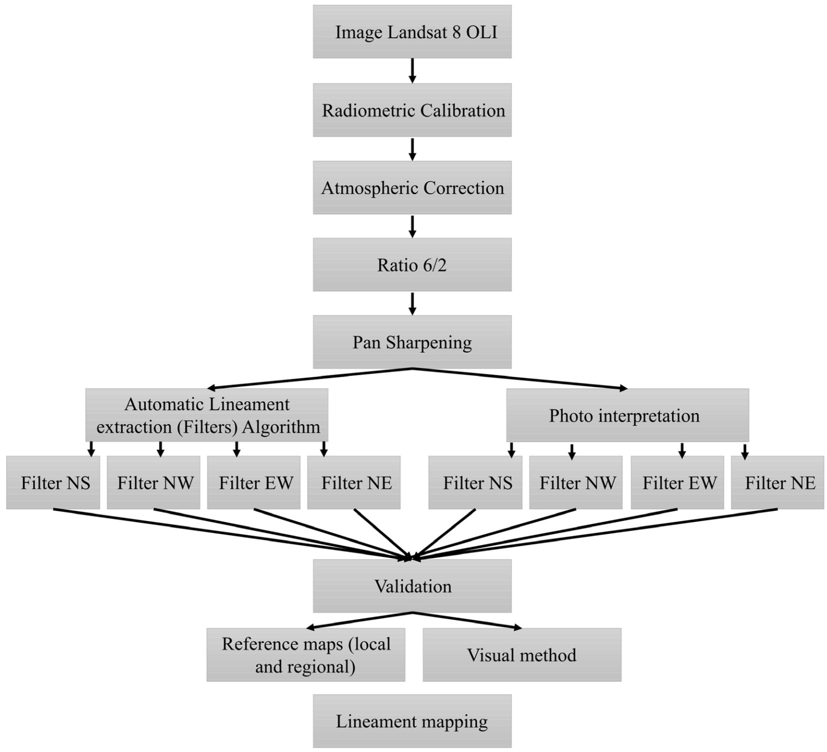

Figure 3. Flowchart showing the main steps of the methodology of tectonic lineament extraction and validation approach.

3.3. Enhancement of Lineaments by Filtering

Directional filters improve lineaments' perception by producing an optical shadow effect adjusted on the image as if it was enlightened by grazing light [79]. Besides, those filters enhance the detection of lineaments, which are not advantaged by the illumination source [80]. We used Sobel operators, widely utilized for lineament extraction and edge detection [81], to enhance the lineaments automatically extracted from directional filters. Sobel filters consist of a selective variety of directional filters using a pair of convolution matrix of 3 * 3, one of them is the other mask rotated by 90˚ (**Table 2**), and is determined based on the distance from the central pixel. In this study, the image used for the filtering is Ratio 6/2.

From these directional filter images (**Figure 4**), the lineaments are automatically extracted, however, the result is not definitive, the work is still incomplete and a visual method must be used before reaching the next step of confirmation and validation.

3.4. Tracing and Validation of Structural Lineaments

After enhancing the edges by directional filtering, we opted for visual inspection [82] [83]. This method allows choosing the significant lineaments of structural origin. Validation of fractures consists mainly of eliminating linear structures related to different parameters (e.g. ridgeline, shade, etc.), so we first compare our map of lineaments with geological and pre-existing structural maps.

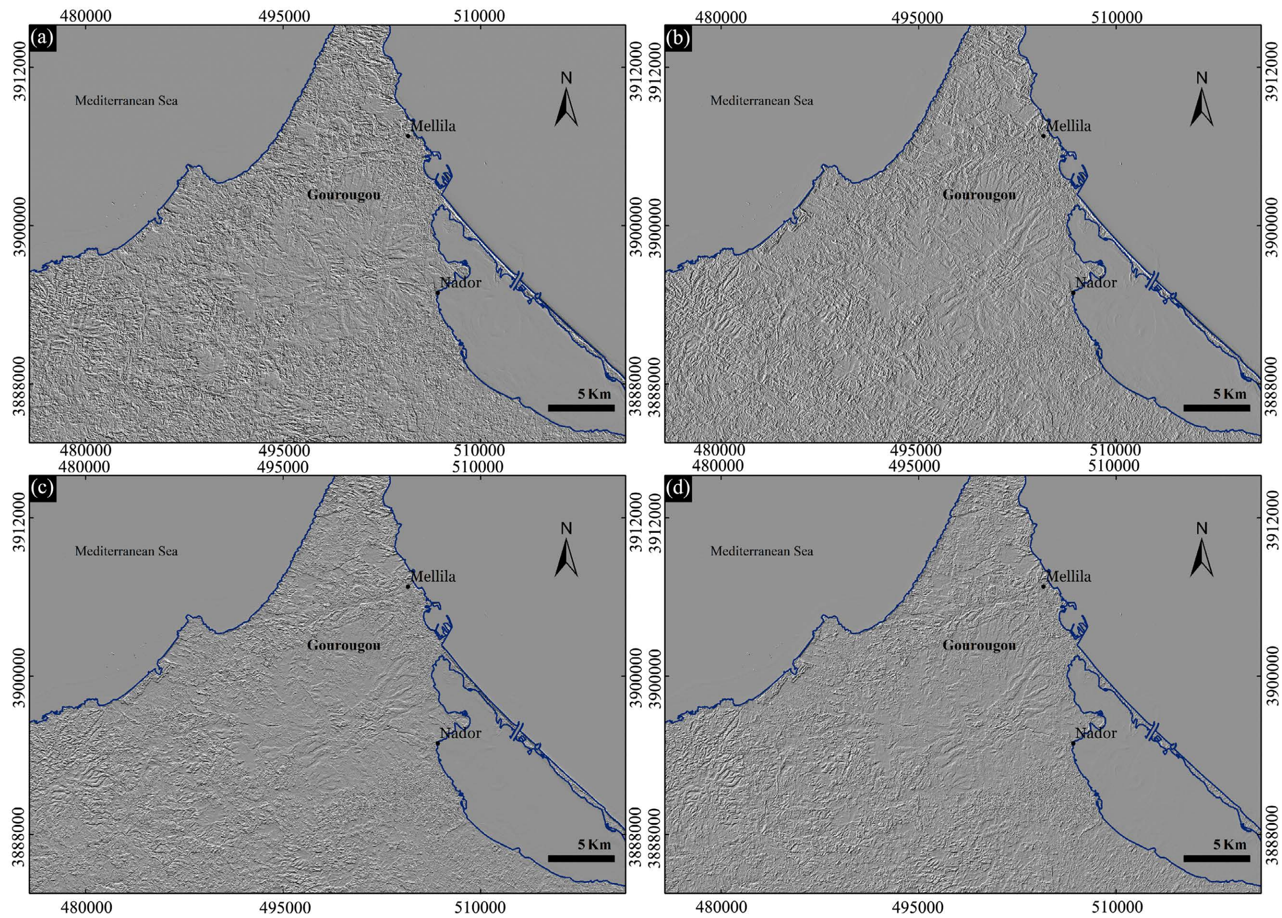

Figure 4. Example of different directional filters applied on the same area (Gourougou). (a) NE, (b) EW, (c) NS, (d) NW.

Table 2. Sobel filters.

3 * 3 Sobel Matrix											
NE-SW			E-W			NW-SE			N-S		
0	1	2	−1	0	1	2	1	2	1	2	1
−1	0	1	−2	0	2	1	0	−1	0	0	0
−2	−1	0	−1	0	1	0	−1	−2	−1	−2	−1

4. Results

Results reveal the existence of more than 4600 lineaments (**Figure 5**, **Figures 6(a)-(c)**, **Figure 7(a)** and **Figure 7(b)**). The length of structures varies and spans from few meters to few kilometers, the longest representable lineament is about 4 kilometers (**Figure 6(a)**). Rose diagram (**Figure 7(b)**) shows that the predominant trending is NE-SW, followed by the E-W, NNE-SSW and N-S trends, respectively, while the weakest represented is the NW-SE trend. Extracted lineaments allowed counting almost 2490 structures striking NE-SW, about 1260 E-W, 360 NNE-SSW, 300 N-S and nearly 190 NW-SE.

A density map (**Figure 8**) is created based on extracted trends, with the aim of

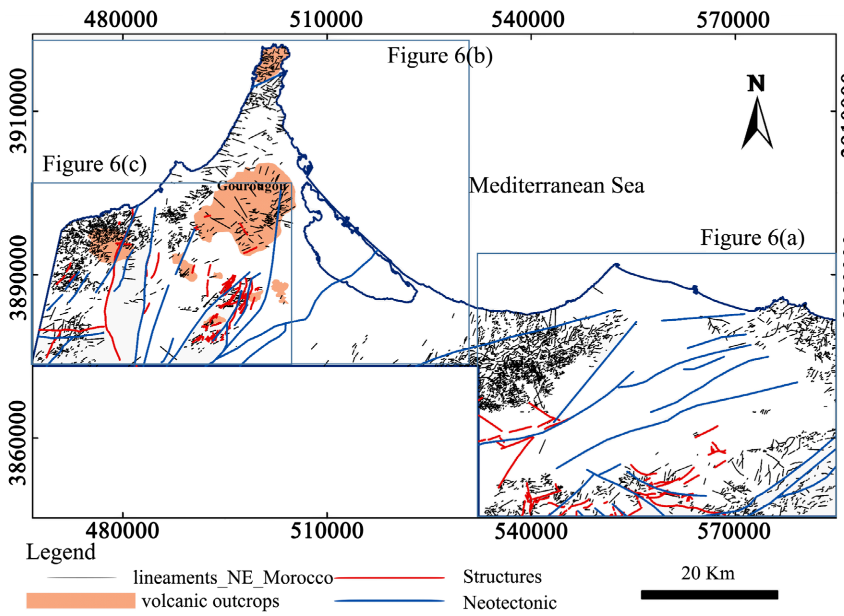

Figure 5. Lineament map of the northeastern Rif. Green squares represent the zoomed areas below.

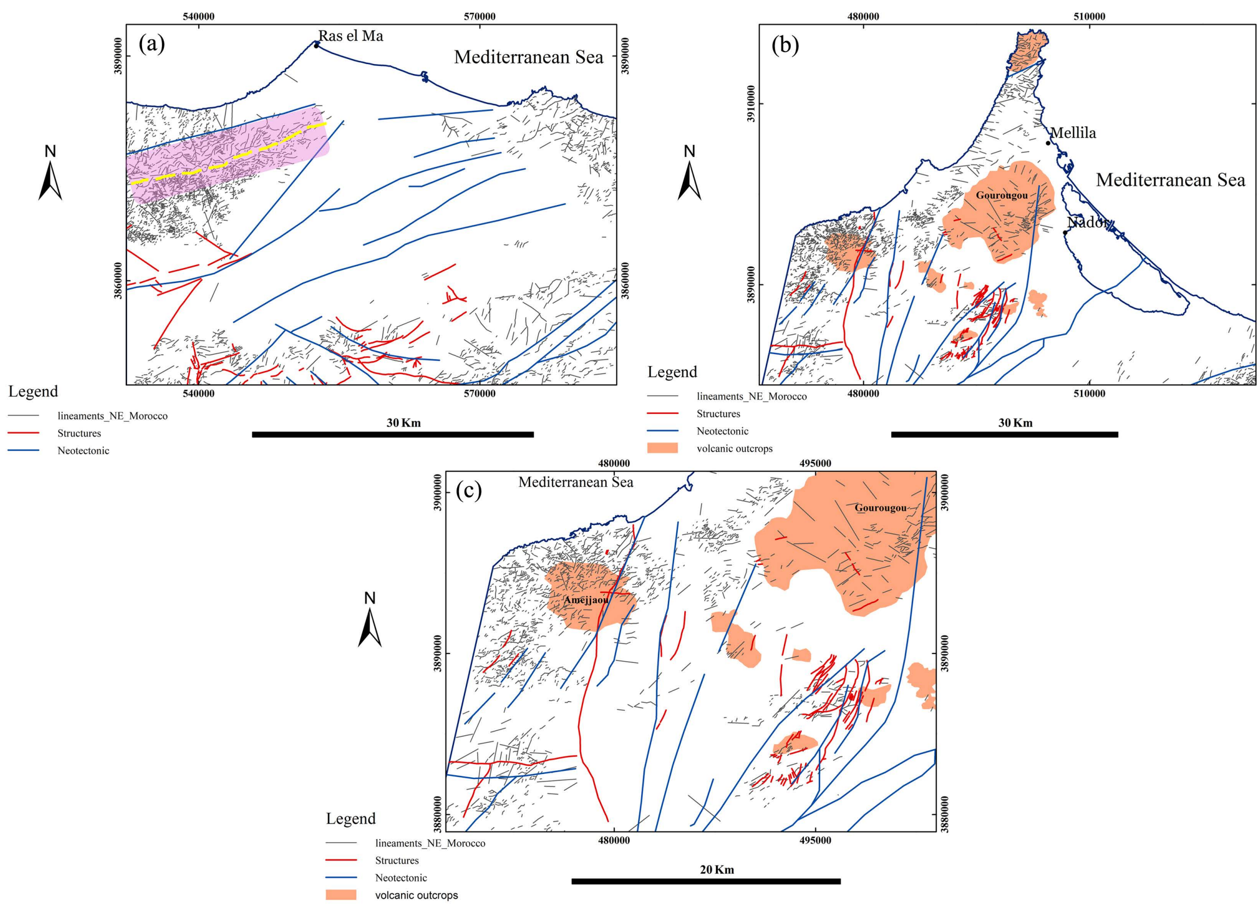

Figure 6. (a) map of lineaments of Zaio-Berkane-Ras el ma regions (yellowish not continued line represents the trend of the lineament drawn by the visual method and the purple shadow refers to the difference between the extracted and the visual trends), (b) map of lineaments of Amejjaou-Nador-Melilla regions, (c) map of lineaments of Seghanghan and Amejaou regions.

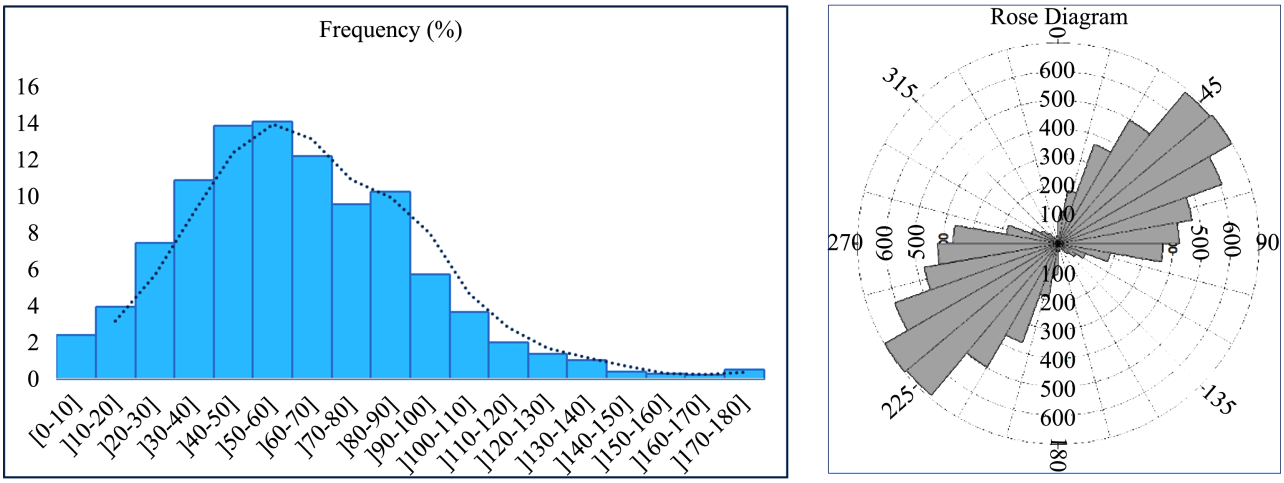

(a) (b)

Figure 7. (a) Length frequency diagram (b) Rose diagram. (2490 NE-SW, about 360 NNE-SSW, 1260 E-W, 300 N-S, 190 NW-SE).

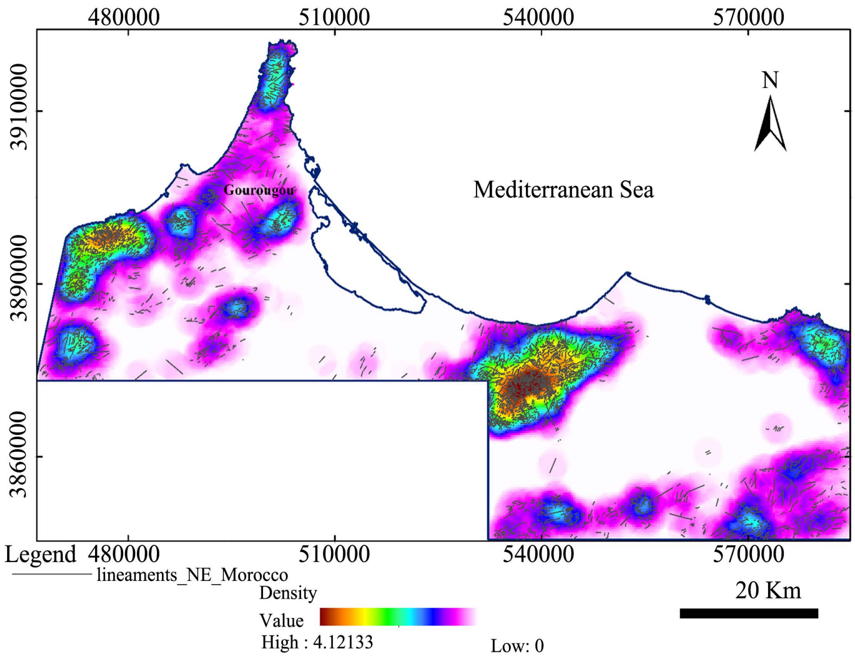

Figure 8. Density map of lineaments in the Northeast of Morocco.

revealing zones with high structural density. Two areas have the highest densities: the first is Kebdana, close to Kariat Arekmane and Ras el Ma, reported in the geological map as formed by Jurassic limestone; the second is Amejjaou, in the west of Seghanghan and Nador, described in the geological map as a part of the Temsamane unit, consisting mainly of Shists. Areas of Nador, Melilla and the coastal limit with Algeria show a high density as well.

Compared to materials used for validation, the number of highlighted structures within the area is more important in this study than the number of linear structures in geologic and structural maps, made based on fieldwork. Mapped lineaments generally correspond to fractures and faults, mainly related to volcanic outcrops, Miocene basins and Jurassic terrains. The fracture is usually a result of breaking a rock in response to stress, if one of the two sides of the fracture moved, it is no longer a simple fracture, but a fault that has a couple of well-known criteria.

Recorded structures in the geological maps of Northeast of Morocco (Kebdani, Seghanghan, Zaio and Berkane) and the Neotectonic map of Morocco are quite the same, although, sometimes, the superimposition is conveyed through several segments and the result is spoiled. This imperfection might be due to satellite images' spatial resolution (30 m) or lineaments' invisibility in these areas.

NE-SW, E-W and N-S trending systems, obtained by processing satellite images, are reported on diagrams showing a similarity to what is described in the literature and to the measurements taken in the field, noting that the N-S trend is weakly represented in the digital processing results.

The validation process of the outputs proves that coupling automatic extraction and visual interpretation methods give better results. Morocco's neotectonic map shows quite a good correlation of structures with what was obtained from the processing methods. Although in the map, features are represented as huge faults and structures, trend and localization of the lineaments are respected in our generated map, with slight differences, yet very logical and acceptable. In fact, structures are represented as several aligned segments with the same direction (**Figure 7(a)**). Despite the good results show a matching correlation with the neotectonic's map, we also note a non-correlation of some other features, which is when areas are covered with vegetation and the satellite images are unable to give accurate responses.

Geological maps of the studied area indicate the presence of several lineaments represented as faults and strike-slip faults. The density of lineaments in geological maps and our generated map is identical. The trends of lineaments are globally coherent and consistent. However, structures in geological maps are sometimes shifted, probably because of projection systems' differences and induced errors. Blanked areas where no lineament is represented (**Figure 5** and **Figure 8**) make the density contrast deeper; this may be explained by the abundance of new constructions and agricultural terrains. These results are therefore highly correlated with the faults' distribution depicted in Neotectonic's and geological maps, with respect to remarks mentioned above.

5. Discussion

The northeast of Morocco represents a very dynamic area. It is related to excessive tectonic regimes since the Late-Miocene with many phases of deformations [84] [85]. The current deformation under the transtensive regime (NNW-SSE to N-S extensive system and NNE-SSW strike-slip faults), in the South of Alboran Ridge and Nekor Basin, is limited by Al-Idrissi fault (**Figure 1(b)**) [86]. Geodetic studies and kinematic models based on magnetic anomalies of the ocean floor show a current convergent movement of plates in Alboran sea, oriented NW-SE with a speed of 4.3 ± 0.5 mm/yr [87]-[93] and a displacement in the Rif belt towards the southwest with a speed of 5.4 ± 1.5 mm/yr. Whereas the regional seismological studies show:

- A NE-SW extension in the Southern Betics, together with strike-slips [94] [95];
- A transtension in the Alboran Sea [95]-[100];
- Strike-slips and transtension in Northern Rif [101] [102].

A polyphase tectonic history, resulting from several successive compressive and distensive phases from Eocene to the present, is well documented in northeastern Rif [103]. It begins with an oligocene tightening phase-oriented N-S, then it continues with a distensive oligo-miocene phase with the same direction N-S linked to the opening of the Alboran sea, and it ends with an overlap of Carbonate thrusts of Alboran Domain "Bokkoya massif" on the Flysch domain in the SSE (**Figure 1(b)**). Finally, the late compressive NNE-SSW Tortonian phase made the last remarkable structures [103] [104] [105] [106]. Since the late Miocene, surface crustal deformation caused kilometric-sized folds and brittle deformation, associated with the development of large strike-slip faults (*i.e.*, the Nekor fault between Al Hoceima and Nador (**Figure 1**)). Faults' pattern in central and eastern Rif is sorted into three groups, two of which are almost orthogonal: one in the NNE-SSW direction, and one in the NS direction, perpendicular to the coastline, and a last one in NW-SE (**Figure 9**) [105] [107] [108] [109] [110].

Figure 9 summarizes the structural evolution of Neogene post-nappe basins of Eastern Rif [70] [107] and shows that different manifestations in Northeast of Morocco are the result of a polyphase tectonic during the Plio-Quaternary:

- Starting with a large period of distension NE-SW oriented from the Tortonian to the Pliocene followed by a compressive episode, oriented N-S during late Tortonian.

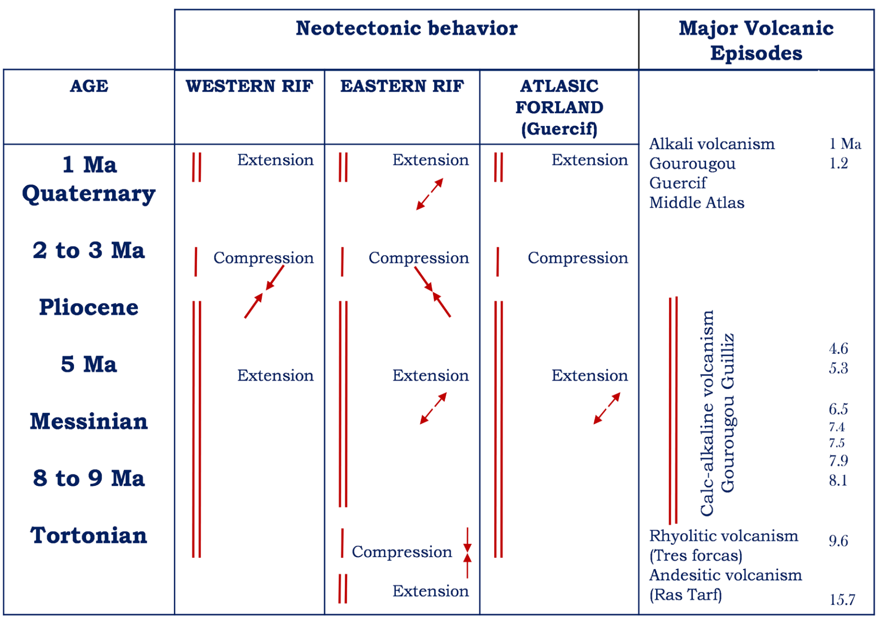

Figure 9. Structural evolution of Neogene post nappe basins of Eastern Rif [70] [107].

- Then, a compressive period, during the upper Pliocene and the early Quaternary, oriented NW-SE and well visible in the Northern border of Gharb and Guercif basins.
- Finally, an extensive period in Quaternary, oriented NE-SW and marked by the most recent features, where the subsidence is well-conserved [107].

Although the E-W trend (poorly cited in literature), identified in this study, is consistent with Belt axis and directions of magnetic anomalies beneath the surface in the northeast part of the Rif [111].

On one hand, previous studies on tectonic movements, lineaments and geospatial information in the northeast of Morocco are very limited. The most recent work dealing with the topic in the area [112] used Landsat image analysis and compared the results with data obtained from radar ERS1-SAR interpretation [113], Spot image analysis [114] and structural field analysis. Four systems of faults were depicted [112]: 1) NE-SW faults with a pattern of en echelon structures (e.g. in the El Aïoun area), recorded during their fieldwork; 2) NW-SE faults; 3) ENE-WSW and E-W faults; 4) faults trending N-S, mainly in Oujda area (Bou Yahi). Although the frame of the current study area and the studied area of the cited work is not exactly the same, it can be considered and used for comparison, as they both share the same geodynamic and geographic settings. Regarding the orientation of present structures, all directions are conformably expressed within the northeast of Morocco; however, the frequency and the dominance are relatively different. NW-SE trending faults, for instance, are the second most dominant faults in the work of [112], while it is the least dominant in this study. This difference might be explained by the dominance of Rif belt structures over Foreland structures within the area (for the current work).

On the other hand, our results were confronted with results of a similar study on NE of Iberia. The latter shows that the bulk of major post-Alpine extensional faults, mainly Neogene, are oriented NW-SE. Secondary structural lineaments, however, show an NNW-SSE trend, running slightly in an oblique way to the main faults [115]. Eruptive fissures and subordinated structural lineaments in northeastern Spain show a pattern, compatible, structurally, with a light dextral transtensional component in two major Neogene faults (Amer and Llora faults), oriented NW-SE [116] [117].

[118] [119] were the first to suggest the idea of magmas taking the way upward in the uppermost crust and subordinated fissures, controlling subsequent eruptions, making this pattern an enhancer to the development of fractures and transport of magma through them [115]. This behaviour apparently is not an exception, though it was described in some other volcanic zones [120]. Within the same area in the NE of Spain, eruptive centres are aligned mainly NW-SE to NNW-SSE, having a sub-parallel trend with lineaments. This orientation might be the reflection of magma-feeding fractures' geometry [115] [121] [122]. A secondary group of volcanic features is elongated NE-SW and ENE-WSW [115].

In the northeast of Morocco, recent volcanic formations towards the south and the southeast of the study area show normal faults trending from N160˚E to

N10˚E [123]. Volcanic flows are aligned along the fissures striking N-S (Oujda region) or exactly at the intersection between N-S normal faults and ENE-WSW strike-slip faults (with a reverse component). The general trend of volcanic outcrops, on a larger scale, is NE-SW to E-W, conformably with the most predominant lineament trend in the northeastern Rif (mainly NE-SW and E-W). This conclusion supports the idea of having a pattern controlling the magma ascension with a preferable direction NE-SW.

6. Conclusions

Combining eye detection with an automatic extraction method using satellite images gave us better results so far. Firstly, it reduces the time of the processing by defining the most likely zones where lineaments could be important in size and distribution. Moreover, it detects the small lineaments, hardly detected onsite. Secondly, structural lineaments are easily selected and rectified once the analysis of detected linear structures is done and suppression of insignificant lineaments (corresponding to roads, rivers, agriculture squares, etc.) is completed. Using only the automatic extraction therefore will not be of high precision and effectiveness.

To summarize, lineament's directions detected from coupling the two methods yield more accurate results. Trends represented in the northeast of Morocco, rating by their abundance within the study area, are NE-SW, E-W, NNE-SSW, N-S and NW-SE. The NE-SW and the E-W trends are the most overriding based on this study, which explains why volcanic outcrops are aligned in the same direction. Northeast of Morocco must have a cracking pattern, similar to the one described in the NE of Spain, leading to a close behavior and hence reflecting the geometry of magma-feeding fractures in north of Morocco. These results have major implications in the undergoing geothermal study within the area, especially in understanding the subsurface flow of thermal fluids in geothermal reservoirs and avoiding serious risks during the geothermal drilling projects.

Acknowledgements

Authors would like to thank the Centre National pour la Recherche Scientifique et Technique (CNRST) for the Research Excellence Scholarship granted to the thesis framing this work. Authors would also like to thank the reviewers for their critical and valuable comments.

Conflicts of Interest

The authors declare no conflicts of interest regarding the publication of this paper.

References

[1] Chindo, M.I. (2011) An Extensive Analysis of Mining in Nigeria Using a GIS. *Journal of Geography and Geology*, **3**, 3-12. https://doi.org/10.5539/jgg.v3n1p3

[2] Ahmadi, H. and Uygucgil, H. (2021) Targeting Iron Prospective within the Kabul Block (SE Afghanistan) via Hydrothermal Alteration Mapping Using Remote Sensing Techniques. *Arabian Journal of Geosciences*, **14**, Article No. 183. https://doi.org/10.1007/s12517-020-06430-3

[3] Eldosouky, A.M., El-Qassas, R.A.Y., Pour, A.B., Mohamed, H. and Sekandari, M. (2021) Integration of ASTER Satellite Imagery and 3D Inversion of Aeromagnetic Data for Deep Mineral Exploration. *Advances in Space Research*, **68**, 3641-3662. https://doi.org/10.1016/j.asr.2021.07.016

[4] Mohamed, H., Hakim, S., Bersi, M., Sami, A., Baher, G., Hamdy, I., Thomas, T. and Mizunaga, H. (2018) 3-D Magnetic Inversion and Satellite Imagery for the Um Salatit Gold Occurrence, Central Eastern Desert, Egypt. *Arabian Journal of Geosciences*, **11**, Article No. 674. https://doi.org/10.1007/s12517-018-4020-6

[5] Tamani, F., Hadji, R., Hamad, A. and Hamed, Y. (2019) Integrating Remotely Sensed and GIS Data for the Detailed Geological Mapping in Semi-Arid Regions: Case of Youks les Bains Area, Tebessa Province, NE Algeria. *Geotechnical and Geological Engineering*, **37**, 2903-2913. https://doi.org/10.1007/s10706-019-00807-2

[6] Lee, S. (2005) Application of Logistic Regression Model and Its Validation for Landslide Susceptibility Mapping Using GIS and Remote Sensing Data. *International Journal of Remote Sensing*, **26**, 1477-1491. https://doi.org/10.1080/01431160412331331012

[7] Rajesh, H.M. (2004) Application of Remote Sensing and GIS in Mineral Resource Mapping—An Overview. *Journal of Mineralogical and Petrological Sciences*, **99**, 83-103. https://doi.org/10.2465/jmps.99.83

[8] Masoud, A. and Koike, K. (2006) Tectonic Architecture through Landsat-7 ETM/SRTM DEM Derived Lineaments and Relationship to the Hydrogeologic Setting in Siwa Region, NW Egypt. *Journal of African Earth Sciences*, **45**, 467-477. https://doi.org/10.1016/j.jafrearsci.2006.04.005

[9] Abdullah, A., Nassr, S. and Ghaleeb, A. (2013) Remote Sensing and Geographic Information System for Fault Segments Mapping a Study from Taiz Area, Yemen. *Journal of Geological Research*, **2013**, Article ID: 20175. https://doi.org/10.1155/2013/201757

[10] Adiri, Z., El Harti, A., Jelloul,i A., Lhissou, R., Maacha, L., Azmi, M., Zouhair, M. and Bachaoui, E.M. (2017) Comparison of Landsat-8, ASTER and Sentinel 1 Satellite Remote Sensing Data in Automatic Lineaments Extraction: A Case Study of Sidi Flah-Bouskour Inlier, Moroccan Anti Atlas. *Advances in Space Research*, **60**, 2355-2367. https://doi.org/10.1016/j.asr.2017.09.006

[11] Ouerghi, S., Elsheikh, R., Aziz, M. and Bouaziz, S. (2017) Structural Interpretation of Lineaments Uses Satellite Images Processing: A Case Study in North-Eastern Tunisia. *Journal of Geographic Information System*, **9**. 440-455. https://doi.org/10.4236/jgis.2017.94027

[12] Azizi, M., Saibi, H. and Cooper, G.R.J. (2015) Mineral and Structural Mapping of the Aynak-Logar Valley (Eastern Afghanistan) from Hyperspectral Remote Sensing Data and Aero-Magnetic Data. *Arabian Journal of Geosciences*, **8**: 10911-10918. https://doi.org/10.1007/s12517-015-1993-2

[13] Jensen, J.R. (2015) Introductory Digital Image Processing: A Remote Sensing Perspective. 4th Edition, Prentice Hall Press, Upper Saddle River.

[14] Pour, A.B., Hashim, M. and Park, Y. (2018) Gondwana-Derived Terranes Structural Mapping Using PALSAR Remote Sensing Data. *Journal of the Indian Society of Remote Sensing*, **46**, 249-262. https://doi.org/10.1007/s12524-017-0673-y

[15] Radaideh, O., Grasemann, B., Melichar, R. and Mosar, J. (2016) Detection and Analysis of Morphotectonic Features Utilizing Satellite Remote Sensing and GIS: An Example in SW, Jordan. *Geomorphology*, **27**, 58-79. https://doi.org/10.1016/j.geomorph.2016.09.033

[16] Ahmadirouhani, R., Rahimi, B., Karimpour, M.H., Shafaroudi, A.M., Najafi, S.A. and Pour, A.B. (2017) Fracture Mapping of Lineaments and Recognizing Their Tectonic Significance Using SPOT-5 Satellite Data: A Case Study from the Bajestan Area, Lut Block, East of Iran. *Journal of African Earth Sciences*, **134**, 600-612. https://doi.org/10.1016/j.jafrearsci.2017.07.027

[17] Masoud, A. and Koike, K. (2017) Applicability of Computer-Aided Comprehensive Tool (LINDA: Lineament Detection and Analysis) and Shaded Digital Elevation Model for Characterizing and Interpreting Morphotectonic Features from Lineaments. *Computers & Geosciences*, **106**, 89-100. https://doi.org/10.1016/j.cageo.2017.06.006

[18] Si Mhamdi, H., Raji, M., Maimouni, S. and Oukassou, M. (2017) Fractures Network Mapping Using Remote sensing in the Paleozoic Massif of Tichka (Western High Atlas, Morocco). *Arabian Journal Geosciences*, **10**, Article No. 125. https://doi.org/10.1007/s12517-017-2912-5

[19] Hamimi, Z., El-Fakharani, A., Emam, A., Barreiro, J.G., Abdelrahman, E. and Abo-Soliman, M.Y. (2018) Reappraisal of the Kinematic History of Nugrus Shear Zone Using PALSAR and Micro-Structural Data: Implications for the Tectonic Evolution of the Eastern Desert Tectonic Terrane, Northern Nubian Shield. *Arabian Journal of Geosciences*, **11**, Article No. 494. https://doi.org/10.1007/s12517-018-3837-3

[20] Takodjou, W.J.D., Ganno, S., Djonthu, L.Y.S., Kouankap, N.G.D., Fossi, D.H., Tchouatcha, M.S. and Nzenti, J.P. (2018) Geostatistical and GIS Analysis of the Spatial Variability of Alluvial Gold Content in Ngoura-Colomines Area, Eastern Cameroon: Implications for the Exploration of Primary Gold Deposit. *Journal of African Earth Sciences*. **142**, 138-157. https://doi.org/10.1016/j.jafrearsci.2018.03.015

[21] Azar, A.P.K., Askari, G., Crispini, L., Pour, A.B., Zoheir, B. and Pradhan, B. (2019) Field and Spaceborne Imagery Data for Evaluation of the Paleo-Stress Regime during Formation of the Jurassic Dike Swarms in the Kalateh Alaeddin Mountain Area, Shahrood, North Iran. *Arabian Journal of Geosciences*, **12**, Article No. 552.

[22] Hamdani, N. and Baali, A. (2019) Fracture Network Mapping Using Landsat 8 OLI Data and Link-Age with the Karst System: A Case Study of the Moroccan Central Middle Atlas. *Remote Sensing in Earth Systems Sciences*, **2**, 1-17. https://doi.org/10.1007/s41976-019-0011-y

[23] Hosseini, S., Lashkaripour, G.R., Moghadas, N.H., Ghafoori, M. and Pour, B.A. (2019) Lineament Mapping and Fractal Analysis Using SPOT-ASTER Satellite Imagery for Evaluating the Severity of Slope Weathering Process. *Advances in Space Research*, **63**, 871-885. https://doi.org/10.1016/j.asr.2018.10.005

[24] Javhar, A., Chen, X., Bao, A., Jamshed, A., Yunus, M., Jovid, A. and Latipa, T. (2019) Comparison of Multi-Resolution Optical Landsat-8, Sentinel-2 and Radar Sentinel-1 Data for Automatic Lineament Extraction: A Case Study of Alichur Area, SE Pamir. *Remote Sensing*, **11**, Article No. 778. https://doi.org/10.3390/rs11070778

[25] Arifin, A., Adnan, N.A. and Abdul Rasam A.R. (2021) Multi-Sensor Assessment of Geological Lineament Detection. *IOP Conference Series*: *Earth and Environmental Science*, **767**, Article ID: 012014. https://doi.org/10.1088/1755-1315/767/1/012014

[26] Céleste, T.S., Hermann, F.D., Gautier, K.P., Eric, D.S., Willy, L. and Elvis, B.W.W. (2021) Comparison of Landsat 8 (OLI) and Landsat 7 (ETM+) Satellite Remote

Sensing Data in Auto-Matic Lineaments Extraction: A Case Study of Nkolezom, Southern Part of Cameroon. *The International Journal of Engineering and Science*, **10**, 24-31.

[27] Khosravi, V., Shirazi, A., Shirazy, A., Hezarkhani, A. and Pour, A.B. (2021) Hybrid Fuzzy-Analytic Hierarchy Process (AHP) Model for Porphyry Copper Prospecting in Simorgh Area, Eastern Lut Block of Iran. *Mining*, **2**, 1-12. https://doi.org/10.3390/mining2010001

[28] Hedayat, B., Ahmadi, M.E., Nazerian, H., Shirazi, A. and Shirazy, A. (2022) Feasibility of Simultaneous Application of Fuzzy Neural Network and TOPSIS Integrated Method in Potential Mapping of Lead and Zinc Mineralization in Isfahan-Khomein Metallogeny Zone. *Open Journal of Geology*, **12**, 215-233. https://doi.org/10.4236/ojg.2022.123012

[29] Akman, A.U. and Tufekçi, K. (2004) Determination and Characterization of Fault Systems and Geomorphological Features by RS and GIS Techniques in the WSW Part of Turkey. *Proceeding of the 20th International Society for Photogrammetry and Remote Sensing Congress*, Istanbul, 12-3 July 2004. http://www.isprs.org/istanbul2004/comm7/papers/205.pdf

[30] Sarup, J., Muthukumaran, M., Nitin, M. and Peshwa, V. (2006) Study of Tectonics in Relation to the Seismic Activity of the Dalvat Area, Nasik District, Maharashtra, India Using Remote Sensing and GIS Techniques. *International Journal of Remote Sensing*, **27**, 2371-2387. https://doi.org/10.1080/01431160500497846

[31] Solomon, S. and Ghebreab, W. (2006) Lineament Characterization and Their Tectonic Significance Using Landsat TM Data and Field Studies in the Central Highlands of Eritrea. *Journal of African Earth Sciences*, **46**, 371-378. https://doi.org/10.1016/j.jafrearsci.2006.06.007

[32] Srivastava, P.K. and Bhattacharya, A.K. (2006) Groundwater Assessment through an Integrated Approach Using Remote Sensing, GIS and Resistivity Techniques: A Case Study from a Hard Rock Terrain. *International Journal of Remote Sensing*, **27**, 4599-4620. https://doi.org/10.1080/01431160600554983

[33] Mountrakis, D., Pavlides, S., Zouros, N., Astaras, T. and Chatzipetros, A. (1998) Seismic Fault Geometry and Kinematics of the 13 May 1995 Western Macedonia (Greece) Earthquake. *Journal of Geodynamics*, **26**, 175-196. https://doi.org/10.1016/S0264-3707(97)00082-3

[34] Ramli, M.F., Yusof, N., Yusoff, M.K., Juahir, H. and Shafri, H.Z.M. (2010) Lineament Mapping and Its Application in landslide Hazard Assessment: A Review. *Bulletin of Engineering Geology and the Environment*, **69**, 215-233. https://doi.org/10.1007/s10064-009-0255-5

[35] Greenbaum, D. (1987) Lithological Discrimination in Central Snowdonia Using Airborne Multispectral Scanner Imagery. *International Journal of Remote Sensing*, **8**, 799-816. https://doi.org/10.1080/01431168708948691

[36] Mathew, J., Jha, V.K. and Rawat, G.S. (2007) Application of Binary Logistic Regression Analysis and Its Validation for Landslide Susceptibility Mapping in Part of Garhwal Himalaya, India. *International Journal of Remote Sensing*, **28**, 2257-2275. https://doi.org/10.1080/01431160600928583

[37] Ricchetti, E. and Palombella, M. (2005) Application of Landsat 7 ETM+ Imagery for Geological Lineament Analysis of Southern Italy. *Proceedings of International Geoscience and Remote Sensing Symposium* (*IGARSS)*, Seoul, 29 July 2005, 5200-5203. https://doi.org/10.1109/IGARSS.2005.1526856

[38] Pradhan, R.P., Singh, R.P. and Buchroithner, M.F. (2006) Estimation of Stress and

Its Use in Evaluation of Landslide Prone Regions Using Remote Sensing Data. *Advances in Space Research,* **37**, 698-709. https://doi.org/10.1016/j.asr.2005.03.137

[39] Pandey, P. and Sharma, L.N. (2019) Comparison of Directional and Non-Directional Filter Techniques for Lineament Extraction Using Landsat-8 OLI to Study Active Tectonics in Parts of North-Western HFT. *Research Journal of Recent Sciences*, **8**, 31-37.

[40] Gupta, R.P. (1991) Digital Image Processing in Remote Sensing Geology. Springer Berlin, Heidelberg, 183-221. https://doi.org/10.1007/978-3-662-12914-2

[41] Sander, P., Minor, T.B. and Chesley, M.M. (1997) Groundwater Exploration Based on Lineament Analysis and Reproducibility Tests. *Groundwater*, **35**, 888-894. https://doi.org/10.1111/j.1745-6584.1997.tb00157.x

[42] Mabee, S.B., Hardcastle, K.C. and Wise, D.U. (1994) A Method of Collecting and Analyzing Line-Aments for Regional Scale Fractured-Bedrock Aquifer Studies. *Groundwater*, **32**, 884-894. https://doi.org/10.1111/j.1745-6584.1994.tb00928.x

[43] Mattauer, M., Tapponnier, P. and Proust, F. (1977) Sur les mécanismes de formation des chaînes intracontinentales. L'exemple des chaînes atlasiques du Maroc. *Bulletin de la Société Géologique de France*, **S7**-**19**, 521-526. https://doi.org/10.2113/gssgfbull.S7-XIX.3.521

[44] Ait Brahim, L., Chotin, P. (1983) Mise en évidence d'un épisode compressif dans les cal-caires plio-quaternaires du bassin de Saiss, Rif, Maroc. *Comptes Rendus de l'Académie des Sciences Paris*, **298**, 1333-1336.

[45] Hoepffner, C. (1987) La tectonique hercynienne dans l'est du Maroc. PhD thesis in Sciences, Université de Strasbourg, Strasbourg, 280 p.

[46] Torbi, A. and Gelard, J.P. (1994) Paléocontraintes enregistrés par la microfracturation, depuis l'Hercynien jusqu'à l'Actuel, dans les Monts du Sud-Est d'Oujda (Meseta oriental, Maroc). *Comptes Rendus de l'Académie des Sciences Paris*, **318**, 131-135.

[47] Tabyaoui, H., Ait Brahim, L., Tahiri, A. and Chotin, P. (1999) Evolution tectono-sédimentaire du N-E du Maroc au cours du Trias supérieur: Apport des données microtectoniques. *Revue de la Géologie Méditerranéenne*, *Marseille*, **26**, 231-243. https://doi.org/10.3406/geolm.1999.1659

[48] Chotin, P., Ait Brahim, L. and Tabyaoui, H. (2000) The Southern Tethyan Margin in North-Eastern Morocco, Sedimentary Characteristics and Tectonic Control. Peri-Tethys Mémoire 5. *Mémoires du Muséum National de l'histoire Naturelle*, *Paris*, **182**, 107-128.

[49] Leprêtre, R., Frizon de Lamotte, D., Combier, V., Gimeno-Vives, O., Mohn, G. and Eschard, R. (2018) The Tell-Rif Orogenic System (Morocco, Algeria, Tunisia) and the Structural Heritage of the Southern Tethys Margin. *BSGF—Earth Sciences Bulletin*, **189**, Article No. 10. https://doi.org/10.1051/bsgf/2018009

[50] Duggen, S., Hoernle, K., Van Den Bogaard, P. and Garbe-Schönberg, A. (2005) Post-Collisional Transition from Subduction to Intraplate-Type Magmatism in the Westernmost Mediterranean: Evidence for Continental-Edge Delamination of Subcontinental Lithosphere. *Journal of Petrology*, **46**, 1155-1201. https://doi.org/10.1093/petrology/egi013

[51] Palomeras, I., Villaseñor, A., Thurner, S., Levander, A., Gallart, J. and Harnafi, M. (2017) Lithospheric Structure of Iberia and Morocco Using Finite-Frequency Rayleigh Wave Tomography from Earthquakes and Seismic Ambient Noise. *Geochemistry*, *Geophysics*, *Geosystems*, **18**, 1824-1840. https://doi.org/10.1002/2016GC006657

[52] Missenard, Y., Zeyen, H., Frizon de Lamotte, D., Leturmy, P., Petit, C., Sebrier, M.

and Saddiqi, O. (2006) Crustal versus Asthenospheric Origin of Relief of the Atlas Mountains of Morocco. *Journal of Geophysical Research*, **111**, Article ID: B03401. https://doi.org/10.1029/2005JB003708

[53] Henandez, J. (1983) Le volcanisme miocène du Rif oriental (Maroc): Géologie, pétrologie et minéralogie d'une province shoshonitique. PhD Thesis in Sciences, Sorbonne University Pierre and Marie Curie Campus, Paris, No. 83-25, 592.

[54] Maury, R.C., Fourcade, S., Coulon, C., El Azzouzi, M., Bellon, H., Coutelle, A., Ouabadi, A., Semroud, B., Megartsi, M., Cotton, J., Belanteur, O., Louni-Hacini, A., Pique, A., Capdevila, R., Hernandez, J. and Rehault, J.P. (2000) Post-Collisional Neogene Magmatism of the Mediterranean Maghreb Margin: A Consequence of Slab Breakoff. *Comptes Rendus de l'Académie des Sciences*, **331**, 159-173. https://doi.org/10.1016/S1251-8050(00)01406-3

[55] Polyak, B.G., Fernàndez, M., Khutorskoy, M.D., Soto, J.I., Basov, I.A., Comas, M.C., Khain, V.Y., Alonso, B., Agapova, G.V., Mazurova, I.S., Negredo, A., Tochitsky, V.O., Rubio, J., Bogdanov, N.A. and Banda, E. (1996) Heat Flow in the Alboran Sea, weStern Mediterranean. *Tectonophysics,* **263**, 191-218. https://doi.org/10.1016/0040-1951(95)00178-6

[56] Missenard, Y. and Cadoux, A. (2011) Can Moroccan Atlas Lithospheric Thinning and Volcanism Be Induced by Edge-Driven Convection? *Terra Nova,* **24**. 27-33. https://doi.org/10.1111/j.1365-3121.2011.01033.x

[57] Negro, F., Sigoyer, J.D., Goffé, B., Saddiqi, O. and Villa, I.M. (2008) Tectonic Evolution of the Betic-Rif Arc: New" Constraints from 40Ar/39Ar Dating on White micas in the Temsamane Units (External Rif, Northern Morocco). *Lithos*, **106**, 93-109. https://doi.org/10.1016/j.lithos.2008.06.011

[58] Dillon, W.P., Robb, J.M., Greene, H.G. and Lucena, J.C. (1980) Evolution of the Continental Margin of Southern Spain and the Alboran Sea. *Marine Geology*, **36**, 205-226. https://doi.org/10.1016/0025-3227(80)90087-0

[59] Berrahma, M. (1982) Volcanisme miopliocene de la partie NW du Massif du Siroua (An-ti-Arias Central, Maroc), étude structurale et pétrologique. PhD Thesis, Université Paris-Sud, Orsay, 152.

[60] Ait Brahim, L., Chotin, P., Tadili, B. and Ramdani, M. (1990) Failles actives dans le Rif central et oriental. *Comptes rendus de l'Académie des Sciences*, **310**, 1123-1129.

[61] Ait Brahim, L. (1985) La zone de fracture trans-Agadir-Nekor: critères géophysiques, don-nées de terrain et analyse de documents "LANDSAT" (Maroc). *Bulletin de l'Institut Scientifique*, **9**, 1-12.

[62] Bellon, H. (1976) Séries magmatiques néogènes et quaternaires du pourtour de la Méditerranée occidentale, comparées dans leur cadre géochronologique. Implications geodynamiques. PhD Thesis in Sciences. Université Paris-Saclay, Bures-sur-Yvette, Orsay No. 1750, 367.

[63] Banda, E. and Ansorge, J. (1980) Crustal Structure under the Central and Eastern Part of the Betic Cordillera. *Geophysical Journal International*, **63**, 515-532. https://doi.org/10.1111/j.1365-246X.1980.tb02635.x

[64] El Bakkali, S., Gourgaud, A., Bourdier, J.-L., Bellon, H. and Gundogdu, N. (1998) Post-Collision Neogene Volcanism of the Eastern Rif (Morocco): Magmatic Evolution through Time. *Lithos*, **45**, 523-543. https://doi.org/10.1016/S0024-4937(98)00048-6

[65] Ait Brahim, L. and Chotin, P. (1983) Résultat de l'analyse de la fracturation des formations "postnappes" du Rif central, depuis Teroual à l'Ouest Jusqu'à Boured à l'Est. *Mines, Géol. et Energie, Rabat, Maroc*, **54**, 210-225.

[66] Ait Brahim, L. and Chotin, P. (1984) Mise en évidence d'un changement de direction de compression dans l'avant-pays rifain (Maroc) au cours du Tertiaire et du Quaternaire. *Bulletin de la Société Géologique de France*, **4**, 681-691. https://doi.org/10.2113/gssgfbull.S7-XXVI.4.681

[67] Aït Brahim, L. and Chotin, P. (1990) Oriental Moroccan Neogene Volcanism and Strike-Slip Faulting. *Journal of African Earth Sciences* (*and the Middle East*), **11**, 273-280. https://doi.org/10.1016/0899-5362(90)90005-Y

[68] Colletta, B. (1977) Evolution néotectonique de la partie méridionale du bassin de Guercif (Maroc oriental). PhD Thesis, Université de Grenoble Alpes, Grenoble, 150.

[69] De Lucas, P. (1978) L'unité chaotique des Kebdana (région de Zaio, Maroc). Relation structurale avec l'avant-pays du Rif Oriental. *Bulletin de la Société Géologique de France*, **S7-20**, 339-343. https://doi.org/10.2113/gssgfbull.S7-XX.3.339

[70] Guillemin, H. and Houzay, J.P. (1982) Le Néogène post-nappes et le Quaternaire du Rif nord-oriental (Maroc). Stratigraphie et tectonique des bassins de Melilla, du Kert, de Boudinar et du piedmont des Kebdana. *Notes et Mémoires du Service Géologique*, **314**, 7-239.

[71] Hervouet, Y. (1985) Géodynamique alpine (Trias-Actuel) de la marge septentrionale de l'Afrique au Nord du Bassin de Guercif (Maroc oriental). PhD Thesis in Sciences, University of Pau et des Pays de l'Adour, Bordeaux, No. 51, 367.

[72] Dutour, A. and Ferrandini, J. (1985) Nouvelles observations néotectoniques dans le Haut-Atlas de Marrakech et le Haouz central (Maroc). *Revue de Géologie Dynamique et de Géographie Physique*, **26**, 285-297.

[73] Ait Brahim, L. (1986) Tectonique messinienne et plio-quaternaire du piedmont septentrional des Kebdana (Rif oriental, Maroc). *4eme Colloque des Bassins Sédimentaires*, Rabat, L'institut scientifique, Rabat, 25.

[74] Harmand, C. and Moukadiri, A. (1986) Synchronisme entre tectonique compressive et volcanisme alcalin: Exemple de la province quaternaire du Moyen-Atlas (Maroc). *Bulletin de la Société Géologique de France*, **2**, 595-603. https://doi.org/10.2113/gssgfbull.II.4.595

[75] Suter, G. (1980) Carte structurale du Rif, 1/500 000. *Notes et Mémoires du Service Géologique*, 245.

[76] Irons, J.R., Dwyer, J.L. and Barsi, J.A. (2012) The Next Landsat Satellite: The Landsat Data Continuity Mission. *Remote Sensing of Environment*, **122**, 11-21. https://doi.org/10.1016/j.rse.2011.08.026

[77] Roy, D.P., Wulder, M.A., Loveland, T.R., C.E., Woodcock, A., R.G., Anderson, M.C., Hel-der, D., Irons, J.R., Johnson, D.M., Kennedy, R., Scambos, T.A., Schaaf, C.B., Schott, J.R., Sheng, Y., Vermote, E.F., Belward, A.S., Bindschadler, R., Cohen, W.B., Gao, F., Hipple, J.D., Hostert, P., Huntington, J., Justice, C.O., Kilic, A., Kovalskyy, V., Lee, Z.P., Lymburner, L., Masek, J.G., McCorkel, J., Shuai, Y., Trezza, R., Vogelmann, J., Wynne, R.H. and Zhu, Z. (2014) Landsat-8: Science and Product Vision for Terrestrial Global Change Research. *Remote Sensing of Environment*, **145**, 154-172. https://doi.org/10.1016/j.rse.2014.02.001

[78] Mwaniki, M., Möller, M. and Schellmann, G. (2015) A Comparison of Landsat 8 (OLI) and Landsat 7 (ETM+) in Mapping Geology and Visualising Lineaments: A Case Study of Central Region Kenya. *International Archives of the Photogrammetry, Remote Sensing and Spatial Information Sciences*, **XL-7/W3**. 897-903. https://doi.org/10.5194/isprsarchives-XL-7-W3-897-2015

[79] Marion, A. (1987) Introduction aux techniques de traitement d'image. Éditions Ey-

rolles, Paris.

[80] Drury, S.A. (1986) Remote Sensing of Geological Structure in Temperate Agricultural Terrain. *Geological Magazine*, **123**, 113-121. https://doi.org/10.1017/S0016756800029770

[81] Ahmadi, H. and Pekkan, E. (2021) Fault-Based Geological Lineaments Extraction Using Remote Sensing and GIS—A Review. *Geosciences*, **11**, Article No. 183. https://doi.org/10.3390/geosciences11050183

[82] Huntington, J.F. and Raiche, A.P. (1978) A Multi-Attribute Method for Comparing Geological Lineament Interpretations. *Remote Sensing of Environment*, **7**, 145-161. https://doi.org/10.1016/0034-4257(78)90044-5

[83] Azman, A.I., Talib, J.A. and Sokiman, M.S. (2020) The Integration of Remote Sensing Data for Lineament Mapping in the Semanggol Formation, Northwest Peninsular Malaysia. *IOP Conference Series*: *Earth and Environmental Science*, **540**, Article ID: 012026. https://doi.org/10.1088/1755-1315/540/1/012026

[84] Bourgois, J., Mauffret, A., Ammar, A. and Demnati, A. (1992) Multichannel Seismic Data Imaging of Inversion Tectonics of the Alboran Ridge (Western Mediterranean Sea). *Geo-Marine Letters*, **12**, 117-122. https://doi.org/10.1007/BF02084921

[85] Do Couto, D. (2014) Evolution géodynamique de la mer d'Alboran par l'étude des bassins sédimentaires. PhD Thesis, Université Pierre et Marie Curie, Paris.

[86] Lafosse, M., d'Acremont, E., Rabaute, A., Estrada, F., Jollivet, C.M., Galindo-Zaldivar, J., Ercilla, G., Alonso, B., Smit, J., Ammar, A., Gorini, C. and Vasquez, J. (2020) Plio-Quaternary Tectonic Evolution of the Southern Margin of the Alboran Basin (Western Mediterranean). *Solid Earth*, **11**, 741-765. https://doi.org/10.5194/se-11-741-2020

[87] DeMets, C., Gordon, R.G., Argus, D.F. and Stein, S. (1994) Effect of Recent revisions to the Geomagnetic Reversal Time Scale on Estimates of Current Plate Motions. *Geophysical Research Letters*, **21**, 2191-2194. https://doi.org/10.1029/94GL02118

[88] McClusky, S., Reilinger, R., Mahmoud, S., Ben Sari, D. and Tealeb, A. (2003) GPS constraints on Africa (Nubia) and Arabia Plate Motions. *Geophysical Journal International*, **155**, 126-138. https://doi.org/10.1046/j.1365-246X.2003.02023.x

[89] Fadil, A., Vernant, P., McClusky, S., Reilinger, R., Gomez, F., Sari, D.B., Mourabit, T., Feigl, K. and Barazangi, M. (2006) Active Tectonics of the Western Mediterranean: Geodetic Evidence for Rollback of a Delaminated Subcontinental lithospheric Slab Beneath the Rif Mountains, Morocco. *Geology*, **34**, 529-532. https://doi.org/10.1130/G22291.1

[90] Tahayt, A., Mourabit, T., Rigo, A., Feigl, K.L., Fadil, A., McClusky, S., Reilinger, R., Ser-roukh, M., Ouazzani-Touhami, A. and Sari, D.B. (2008) Mouvements actuels des blocs tec-toniques dans l'arc BéticoRifain à partir des mesures GPS entre 1999 et 2005. *Comptes Rendus Geoscience*, **340**, 400-413. https://doi.org/10.1016/j.crte.2008.02.003

[91] Vernant, P., Fadil, A., Mourabit, T., Ouazar, D., Koulali, A., Davila, J.M., Garate, J., McClusky, S. and Reilinger, R. (2010) Geodetic Constraints on Active Tectonics of the Western Mediterranean. Implications for the Kinematics and Dynamics of the Nubia-Eurasia Plate Boundary Zone. *Journal of Geodynamics*, **49**, 123-129. https://doi.org/10.1016/j.jog.2009.10.007

[92] Argus, D.F., Gordon, R.G. and DeMets, C. (2011) Geologically Current Motion of 56 Plates Relative to the No-Net-Rotation Reference Frame. *Geochemistry, Geophysics, Geosystems*, **12**, Article ID: Q11001.

https://doi.org/10.1029/2011GC003751

[93] Koulali, A., Ouazar, D., Tahayt, A., King, R.W., Vernant, P., Reilinger, R.E., McClusky, S., Mourabit, T., Davila, J.M. and Amraoui, N. (2011) New GPS Constraints on Active Deformation along the Africa-Iberia Plate Boundary. *Earth and Planetary Science Letters*, **308**, 211-217. https://doi.org/10.1016/j.epsl.2011.05.048

[94] Martínez-Martínez, J.M., Booth-Rea, G., Azañón, J.M. and Torcal, F. (2006) Active Transfer Fault Zone Linking a Segmented Extensional System (Betics, Southern Spain): Insight into Heterogeneous Extension Driven by Edge Delamination. *Tectonophysics*, **422**, 159-173. https://doi.org/10.1016/j.tecto.2006.06.001

[95] Stich, D., Serpelloni, E., Mancilla, D.L.F. and Morales, J. (2006) Kinematics of the Iberia-Maghreb Plate Contact from Seismic Moment Tensors and GPS Observations. *Tectonophysics*, **426**, 295-317. https://doi.org/10.1016/j.tecto.2006.08.004

[96] Comas, M.C., García-Dueñas, V. and Jurado, M.J. (1992) Neogene Tectonic Evolution of the Alboran Sea from MCS data. *Geo-Marine Letters*, **12**, 157-164. https://doi.org/10.1007/BF02084927

[97] Watts, A.B., Piatt, J.P. and Buhl, P. (1993) Tectonic Evolution of the Alboran Sea Basin. *Basin Research,* **5**, 153-177. https://doi.org/10.1111/j.1365-2117.1993.tb00063.x

[98] Morel, J.L. and Meghraoui, M., (1996) Goringe-Alboran-Tell Tectonic Zone: A Transpression System along the Africa-Eurasia Plate Boundary. *Geology*, **24**, 755-758. https://doi.org/10.1130/0091-7613(1996)024%3C0755:GATTZA%3E2.3.CO;2

[99] Lonergan, L. and White, N. (1997) Origin of the Betic-Rif Mountain Belt. *Tectonics*, **16**, 504-522. https://doi.org/10.1029/96TC03937

[100] Faccenna, C., Piromallo, C., Crespo-Blanc, A., Jolivet, L. and Rossetti, F. (2004) Lateral Slab Deformation and the Origin of the Western Mediterranean Arcs: Arcs of the Mediterranean. *Tectonics,* **23**, Article ID: TC1012. https://doi.org/10.1029/2002TC001488

[101] Moratti, G., Piccardi, L., Vannucci, G., Belardinelli, M.E., Dahmani, M., Bendkik, A. and Chenakeb, M. (2003) The 1755 "Meknes" Earthquake (Morocco): Field Data and Geodynamic Impli-Cations. *Journal of Geodynamics*, **36**, 305-322. https://doi.org/10.1016/S0264-3707(03)00052-8

[102] Tahayt, A., Feigl, K.L., Mourabit, T., Rigo, A., Reilinger, R., McClusky, S., Fadil, A., Berthi-er, E., Dorbath, L., Serroukh, M., Gomez, F. and Ben Sari, D. (2009) The Al Hoceima (Morocco) Earthquake of 24 February 2004, Analysis and Interpretation of Data from ENVISAT ASAR and SPOT5 Validated by Ground-Based Observations. *Remote Sensing of Environment*, **113**, 306-316. https://doi.org/10.1016/j.rse.2008.09.015

[103] Poujol, A. (2014) Analysis of the Rif Mountain Present-Day Deformation (Morocco): A Mor-Photectonic Approach. PhD Thesis in Geosciences, University of Montpellier 2, Montpellier

[104] Andrieux, J. (1971) La structure du Rif central: étude des relations entre la tectonique de compression et les nappes de glissement dans un tronçon de la chaîne alpine. Editions du Service géologique du Maroc, Rabat.

[105] Azzouz, O. (1992) Lithostratigraphie et tectonique hercynienne des terrains paléozoïques ghomarides du Massif des Bokoya (Rif Interne, Maroc). PhD Thesis, Faculty of Sciences Sciences, Mohammed V University in Rabat, Rabat, 208.

[106] d'Acremont, E., Gutscher, M.A., Rabaute, A., Mercier D.L.B., Lafosse, M., Poort, J., Ammar, A., Tahayt, A., Le Roy, P., Smit, J., Do Couto, D., Cancouët, R., Prunier, C.,

Ercilla, G. and Gorini, C. (2014) High-Resolution Imagery of Active Faulting Offshore Al Hoceima, Northern Morocco. *Tectonophysics*, **632**, 160-166. https://doi.org/10.1016/j.tecto.2014.06.008

[107] Tesson, M. and Gensous, B. (1989) Les bases d'une stratigraphie sismique du Neogene post-nappes en mer d'Alboran, au large du Maroc. Implications structurales et paleogeographiques. *Journal of African Earth Sciences*, **9**, 421-433. https://doi.org/10.1016/0899-5362(89)90026-2

[108] Chalouan, A., Benmakhlouf, M., Mouhir, L., Ouazani-Touhami, A., Saji, R. and Zaghloul, M.N. (1995) Les étapes tectoniques de la structuration alpine du Rif interne (Maroc). *Actes Du IVème Colloque SECEG et SNED*, Seville, 163-191.

[109] Ait Brahim, L., Nakhcha, C., Tadili, B., El Mrabet, A. and Jabour, N. (2004) Structural Analysis and Interpretation of the Surface Deformations of the February 24th, 2004 Al Hoceima Earth-Quake. European-Mediterranean Seismological Centre, Bruyère-le Châtel, 110, 10. http://www.emsc-csem.org

[110] Jabour, N., Kasmi, M., Menzhi, M., Birouk, A., Hni, L., Hahou, Y., Timoulali, Y. and Badrane, S. (2004) The February 24th, 2004 AL Hoceima Earthquake. European-Mediterranean Seismological Centre, Bruyère-le Châtel. http://www.emsc-csem.org

[111] El Azzab, D. and Feinberg, A. (2004) Investigation géomagnétique au Maroc Nord-oriental: Implications géodynamiques. Geomagnetic Investigation in Northeastern Morocco: Geodynamic Implications. Colloque Anne Faure-Muret. Rabat.

[112] El Hammichi, F., Tabyaoui, H., Chaouni, A., Ait Brahim, L. and Chotin, P. (2006) Mio-Pliocene Tectonics in Moroccan Rifian Foreland: Coexistence of Compressive and Extensional Structures. *Revista de la Sociedad Geológica de España*, **19**, 143-152.

[113] Tabyaoui, H. and Ait Brahim, L. (1997) Apport de l'imagerie radar SAR-ERS-1 à la cartogra-phie des structures tectoniques du Maroc oriental. *Actes du 14ème colloque des Bassins sédimentaires marocains*, Kénitra, 24-27 September 1997, 348-350.

[114] Ait Brahim, L., Tabyaoui, H., Chotin, P. and Gelard, J.P. (1994) Apport des données satellitaires Spot-XS contrôlées par une étude de terrain à l'élaboration de la carte géologique des monts de Taourirt-Oujda au 1/200000. *Actes 12ème Colloque Bassins Sédimentaires Marocains*, Casablanca, 29 September-2 October 1994, 10-11.

[115] Bolos, X., Marti, J., Becerril, L., Planaguma, L., Grosse, P. and Barde-Cabusson, S. (2015) Volcano-Structural Analysis of La Garrotxa Volcanic Field (NE Iberia): Implications for the Plumbing System. *Tectonophysics*, **642**, 58-70. https://doi.org/10.1016/j.tecto.2014.12.013

[116] Zarroca, M., Linares, R., Bach, J., Roqué, C., Moreno, V., Font, L. and Baixeras, C. (2012) Integrated Geophysics and Soil Gas Profiles as a Tool to Characterize Active Faults: The Amer Fault Example (Pyrenees, NE Spain). *Environmental Earth Sciences*, **67**, 889-910. https://doi.org/10.1007/s12665-012-1537-y

[117] Fleta, J., Santanach, P., Goula, X., Martínez, P., Grellet, B. and Masana, E. (2001) Preliminary Geologic, Geomorphologic and Geophysical Studies for the Paleoseismological Analysis of the Amer Fault (NE Spain). *Netherlands Journal of Geosciences,* **80**, 245-253. https://doi.org/10.1017/S0016774600023866

[118] Goula, X., Olivera, C., Fleta, J., Grellet, B., Lindo, R., Rivera, L.A., Cisternas, A. and Carbon, D. (1999) Present and Recent Stress Regime in the Eastern Part of the Pyrenees. *Tectonophysics,* **308**, 487-502. https://doi.org/10.1016/S0040-1951(99)00120-1

[119] Olivera, C., Fleta, J., Susagna, T., Figueras, S., Goula, X. and Roca, A. (2003) Seismicity and Recent Deformations in the Northeastern of the Iberian Peninsula. *Física de la Tierra*, **15**, 111-114.

[120] Karakhanian, A., Djrbashian, R., Trifonov, V., Philip, H. and Arakelian, S. (2002) Holocene-Historical Volcanism and Active Faults as Natural Risk Factors for Armenia and Adjacent Countries. *Journal of Volcanology and Geothermal Research*, **113**, 319-344. https://doi.org/10.1016/S0377-0273(01)00264-5

[121] Tibaldi, A. (1995) Morphology of Pyroclastic Cones and Tectonics. *Journal of Geophysical Research*, **100**, 24521-24535. https://doi.org/10.1029/95JB02250

[122] Corazzato, C. and Tibaldi, A. (2006) Fracture Control on Type, morphology and Distribution of Parasitic Volcanic Cones: An Example from Mt. Etna, Italy. *Journal of Volcanology and Geothermal Research,* **158**, 177-194. https://doi.org/10.1016/j.jvolgeores.2006.04.018

[123] Chotin, P. and Brahim, L. (1988) Transpresion et magmatisme Néogène-Quaternaire dans le Maroc oriental. *Comptes Rendus de l'Académie des Sciences Paris*, **306**, 1479-1485.